Mechanism of high *n*-type conduction in nitrogen-doped nanocrystalline diamond

Somnath Bhattacharyya
Department of Physics and Material Science Programme, Indian Institute of Technology, Kanpur, 208016, India
(Received 3 July 2003; revised manuscript received 21 June 2004; published 16 September 2004)

Dramatic enhancement of the *n*-type conductivity of nanocrystalline diamond films by introducing up to 0.2 at. % of nitrogen into the film has been reported. Previously, there were some theoretical predictions about the change of electronic structure of the films by nitrogen incorporation, but the origin of the enhanced conductivity is still not clearly understood. In this article the mechanism of high conductivity and the change of the electronic structure by nitrogen incorporation is investigated by low-temperature conductivity and other supporting measurements. It is shown that nitrogen induces percolative paths in the grain boundary regions and there is an increase in the density of states at the Fermi level that helps increase the conductivity. Low-temperature conductivity has been explained from a change over from Arrhenious behavior to Efros-Shklovokii–Pollak–Mott variable range hopping conductivity. Using a model combining band and hopping conduction electrical conductivity of highly doped samples over wide range of temperature has been explained. This approach also helps us to improve the understanding of the electronic structure and transport of conducting amorphous carbon by resolving some typical problems in the analysis of temperature dependent conductivity.

DOI: 10.1103/PhysRevB.70.125412 PACS number(s): 73.61.Jc, 72.20.−i, 71.55.Jv, 73.20.Hb

I. INTRODUCTION

Recently an enhancement of electrical conductivity of nanocrystalline diamond (NCD) films has been attempted by the incorporation of nitrogen.[1] The reason behind this attempt was based on the idea that nitrogen would be an ideal *n*-type dopant for diamond and related materials. Subsequent to this it has been understood that successful nitrogen doping of single-crystal diamond was quite difficult.[2–4] Because of a high degree of localization of the N wave function, nitrogen behaves as a deep impurity center in diamond, 1.7 eV below the conduction band (CB). Nitrogen in diamond (also in microcrystalline diamond) prefers to form bonds with three neighboring carbon atoms occupying a three-coordinated substitutional site distorted along the (111) direction with two of its electrons acting as a lone pair orbital making doping difficult.[3,4] The degree of disorder is very high in diamondlike (DLC) and tetrahedral amorphous carbon (ta-C) producing tailing of bands in the pseudogap region and thus a substitutional doping of these materials is found to be difficult.[5–7] On the other hand, UNCD can be grown as phase pure diamond, where the degree of disorder can be quite low and confined only to thin (0.2–0.4 nm) grain boundary (GB) regions and hence the effective defect density of state in the band gap region of this mixed phase should be very low making nitrogen doping of NCD feasible.[1] Though high "*n*-type" conductivity has been shown in N-NCD films its origin has not been explained.[1]

Concerning electrical transport doped diamond has been considered as an ideal material for studying hopping conduction.[8] The low-temperature conductivity of *p*-type diamond and related materials has been studied for over fifty years. These data have been tried to fit using various models such as impurity conduction, variable range hopping, multiphonon hopping, etc.[8] However, a linear fit using a particular mechanism throughout the range of measurement was found to be impossible. There is no detailed report available in nanocrystalline diamond in this regard and, therefore, we present this paper based on the conduction of disordered carbon at the grain boundary regions. We analyze the temperature-dependent conductivity of the amorphous carbon at the GB using various standard mechanisms of disordered materials and finally suggest some modification in the present context.

In a disordered system the resistivity as a function of temperature (T) can in general be expressed as $\rho = \rho_0 \exp(-T_m/T)^m$, where the value and sign of m determine the electrical properties of a material.[9] Coulomb interaction in disordered system with strongly localized electronic states plays an important role reducing the single particle density of states (DOS) near the E_F. Efros-Shklovoskii suggested a hopping conduction different than Mott's variable range hopping (VRH) ($m=1/4$), where m in the resistivity expression is $1/2$.[10] It was proposed that long-range unscreened Coulomb repulsion between the electrons in the localized states reduced the single-particle DOS near the E_F. As a result of zero temperature DOS at the E_F is zero but finite at other energies. This distribution of the DOS opens up a gap called Coulomb gap or soft gap. In contrary, Pollak suggested that low-energy excitation could not be described by noninteracting one-electron hopping and the inclusion of many electron effects further reduced the DOS near E_F and opened up a hard gap.[11] In this case, temperature-dependent resistivity follows $\ln \rho$ vs $1/T$, where $m=1$. This means that the exponent m is higher than $\frac{1}{2}$ and ρ is more temperature dependent. There still remains some controversies related to the Coulomb gap as there are more than one type of cross over from Mott $T^{-1/4}$ VRH to $T^{-\nu}$ VRH with the exponent ν considerably greater than $1/2$. This exponent may tend to 1 or remain smaller than 1 but greater than $\frac{1}{2}$. This kind of crossover has been seen in many materials, such as ion implanted Si:P, Si:B, and heavily boron doped synthetic diamond.[12,13] By the variation of temperature we want to check this crossover in nanocrystalline diamond samples doped with different nitrogen concentration. To our knowledge, this kind of a system-

atic study has rarely been performed in diamond or related materials except for at a particular doping concentration[13] and in nanocrystalline diamond films. We would like to study the crossover of the region with $m=1/4-1/2$ or $m=1$ in the present system, nitrogen doped nanocrystalline diamond.

The motivations of the paper are as follows. (i) To correlate the hopping distance with the mean separation of the dopants from proper fittings of the experimental data. (ii) Change of hopping distance and energy range of the mobility edge with temperature. (iii) Change of hopping distance, energy range, and DOS at the E_F with doping concentration. (iv) Estimation of the soft and hard gap, if any. (v) The possibility of the coexistence of band and hopping conduction to fit conductivity over a wide range of temperature. Theoretical predictions for nitrogen doping in the NCD films will be discussed to explain these experimental observations.

II. EXPERIMENTAL

The NCD samples were prepared from a mixture of argon (99 sccm) and methane (1 sccm) in a commercial microwave plasma chemical vapor deposition (MPCVD) system with a varying flow rate of nitrogen (0 to 20 sccm).[1] These films were deposited on *n*-type Si wafer as well as on fused SiO_2 substrate at 100 Torr pressure, 700 W microwave power, and 800 °C substrate temperature.[1] The deposited films were about one micron thick. The microstructure of the films was studied by high-resolution transmission electron microscopy (HRTEM) and the nitrogen atomic percentage in the films was determined by secondary ionization mass spectroscopy (SIMS).[1,14]

Electrical conductivity of the films deposited on fused quartz substrates was measured from 300 K down to 4.2 K in a helium cryostat.[1] For ac conductivity measurements precleaned and heavily doped Si (*n*-type) substrates were used. Frequency-dependent (ac) conductivity of the films deposited on $n-$Si substrates in a sandwich configuration was performed (between 100 Hz and 2 MHz) on an impedance analyzer at room temperature. Electron spin resonance (ESR) measurements have been carried out in an *X*-band spectrometer (Bruker) at variable temperatures down to 77 K (4.2 K for some of the samples). The spin density has been determined using the signal of DPPH (1,1-diphenyl-2-picrylhydrazyl) as a calibration reference.

III. RESULTS

The UNCD samples prepared in the nitrogen free atmosphere were found to be as good insulating materials and therefore, performing temperature-dependent conductivity measurement at low temperature was rather difficult. Upon introduction of nitrogen the conductivity increases very rapidly giving a difference of more than 4 orders in the samples grown with 0.5 and 20 % N_2, as illustrated in Figs. 1(a) and 1(b).[1,14] The room-temperature resistivity for the films grown at 20% N_2 was as low as 3.7 mΩ cm for 20% N_2. This value is much lower than the lowest value reported in both *p*- and *n*-type diamond and related amorphous carbon films.[15,16] It was found that the nitrogen atomic concentration in the films

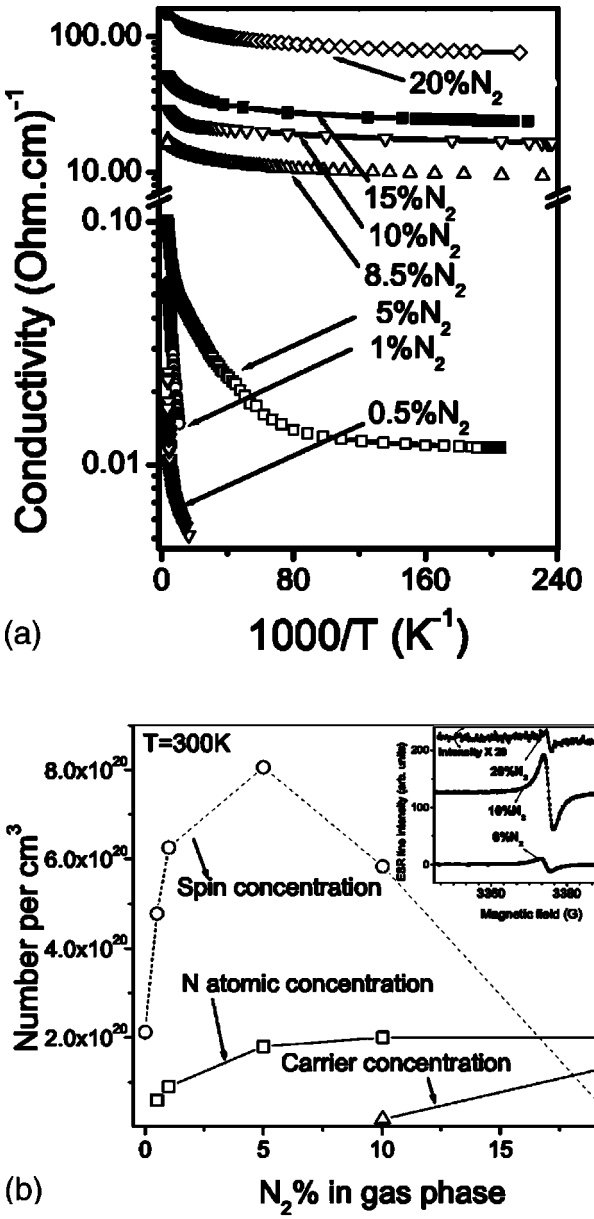

FIG. 1. (a) Variation of conductivity with temperature of NCD samples prepared with different nitrogen concentration. (b) Variation of room temperature conductivity, spin density, and nitrogen atomic concentration with nitrogen gap percentage in the plasma. Inset: Typical ESR peak of NCD films. (See Refs. 1 and 14 for details.)

initially increases up to 5% N_2 in the plasma and beyond that it remains constant unlike the conductivity [Fig. 1(b)]. The spin density increases more than five times in the 5% N_2 samples compared to 0% N_2. Beyond that nitrogen level the spin density decreases with the nitrogen concentration in the plasma [Fig. 1(b)]. Details of the variation of spin concentration will be given elsewhere.[14] With the decrease of temperature, conductivity of all samples were found to decrease but the relative change of the value of conductivity between 300 and 4.2 K was shown to decrease with the increase of nitrogen concentration [Fig. 1(a)]. The temperatures dependency of the conductivity of the NCD films can be analyzed in terms of conduction through the high concentration of

TABLE I. Calculated parameters based on an Arrhenious plot.

N_2% (plasma)	N_{at} (cm^{-3})	$r_{N\text{-}N}$ (Å)	σ_0 (Ohm cm)	E_{act} (low T)	E_{act} (high T)	Comments
0.5	6×10^{19}	15.9	59 (200–140 K) 101 (101–60 K)	3.8 meV (136–60 K)	10.1 meV (210–160 K), 72.0 meV (300 K)	Activated conduction
1.0	9×10^{19}	13.9	7 (226–160 K) 11 (160–100 K)	15.1 meV (160–120 K)	21.6 meV (226–160 K), ~25 meV (300 K)	Hopping conduction

grain boundaries present in the films. Doping of UNCD films appears to be different from the *p*-doped diamond where a clear distinction between the band conduction, hopping, and metallic conduction was observed. Therefore, the increase in conduction can be assigned to the grain boundary (or the interface between diamond grains and the grain boundary regions, see Sec. IV). In the following subsection we discuss on the temperature-dependent conductivity by hopping conduction and percolation through the grain boundary.

Although several researchers explained the temperature-dependent conductivity of microcrystalline and single crystal diamond in terms of different conductivity mechanisms a proper fitting of the conductivity over wide range of temperature seems was not found.[4,15–17] The conductivity as a function of inverse of temperature could not be truly fitted in the entire range of measurements (300–4.2 K) as a linear fit, in general, as a combination of three exponential decay functions expressed as $\sigma=\sigma_{band}\exp(-E_{band}/kT)+\sigma_{imp}\times\exp(-E_{imp}/kT)+\sigma_{hopp}\exp(-E_{hopp}/kT)$ using the model of a nondegenarately doped semiconductor.[15,18] Only for 0.5% (and somewhat for 1% N_2) film this expression seems to hold good and the activation energy calculated appears to be very small (a few meV only) also, see Table I and Fig. 2. From the conductivity data it is clear that for 0.5% N_2 sample conduction is activated $[\rho=\rho_0\exp(-E_{act}/kT)]$ in two different temperature regimes: 60–136 K and 160–210 K with activation energies (E_{act}) 3.8 and 10 meV, respectively (Fig. 2 and Table I). These small values of activation energies are supported by previous works,[18] where E_F is found somewhere within the mobility gap and close to the conduction band. At the low temperatures the conduction arises from the carriers being excited into the localized states at the band edges or hopping or tunneling between localized states (such as sp^2 clusters) near the E_F (particularly for the 1% N_2 sample). A

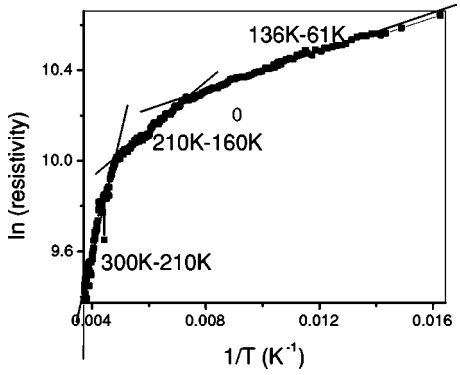

FIG. 2. Arrhenious plot of resistivity of the 0.5% N_2 sample shows activated behavior of conduction.

larger activation energy of ~72 meV has been noticed near to room temperature due to the transition between the delocalized states. A fit of the hopping conduction for this sample deviates from linearity and establishes the presence of a small finite gap. From the optical absorption data of these samples the presence of an energy gap could be verified (not shown here[14]).

Determination of the activation energy from a wide temperature range was found to be difficult and a plot of local gradient of logarithmic plot of conductivity as $E_{act'}(E)=-kd[\ln\sigma(T)/d(1/T)]$ was suggested.[16] By plotting E_{act} with respect to temperature it was found that E_{act} was not a constant but increased with temperature.[16] Recently, Koos *et al.* also followed the same methodology and found a continuous change of $\ln\sigma$ with $1/T$ and suggested that it was due to broad distribution of band tail states where the mobility edge was not sharp.[16] It is worth noting that the presently investigated samples are free from these problems of interpretation. Without taking this kind of approach of the fit of derivative of $\ln\sigma$ with $1/T$ we can clearly see the decrease of E_{act} (E) in the 0.5% N_2 (and also 1% N_2 samples establishing an activated conduction.

In practice, the temperature-dependent resistivity of the 1% N_2 sample can be plotted using different mechanisms. Figure 3(a) shows that an Arrhenious type of resistivity $[\rho=\rho_0\exp(-E_{act}/kT)]$ with at least two distinct slopes with activation energies 21.6 and 15.1 meV, respectively, within temperature ranges 225–160 K and also 160–100 K [Fig. 3(a)]. Therefore, the value of activation energy near room temperature decreases with the increase of nitrogen concentration in the films. However, it is difficult to compare the data from the low-temperature region where an opposite trend has been seen. The change of slope of this curve indicates that there may be other mechanisms rather than activated behavior. Moreover, the hopping mechanism of Efros and Mott's VRH conduction also gave a linear fit over the entire temperature range for the 1% N_2 sample [Fig. 3(b)]. Mott's $T^{-0.25}$ law $[\rho=\rho_0\exp(-T_{1/4}/T)^{0.25}]$ holds good throughout the temperature range and we calculate R_{hopp} and DOS at E_F as follows. Note that we do not have data down to 4.2 K for this sample having low conductance. Thus, in the low-temperature range a possibility of Arrhenious type conduction or Efros type Coulomb gap cannot be ignored. From the atomic concentration of nitrogen (N_{at}) in the films (from SIMS data) the mean distance between nitrogen impurity has been calculated as $r_{N\text{-}N}=[3/4\pi N_{at}]^{1/3}$ and the corresponding Coulomb interaction is $w=e^2/(kr_{N\text{-}N})$ [Table I]. Similarly, following the VRH theory the DOS at E_F was calculated as $g_F=N_{at}/w$. From the fit of the line ln(resistivity) and $T^{-0.25}$ the constant term $T_{1/4}$ can be deduced and compared with the

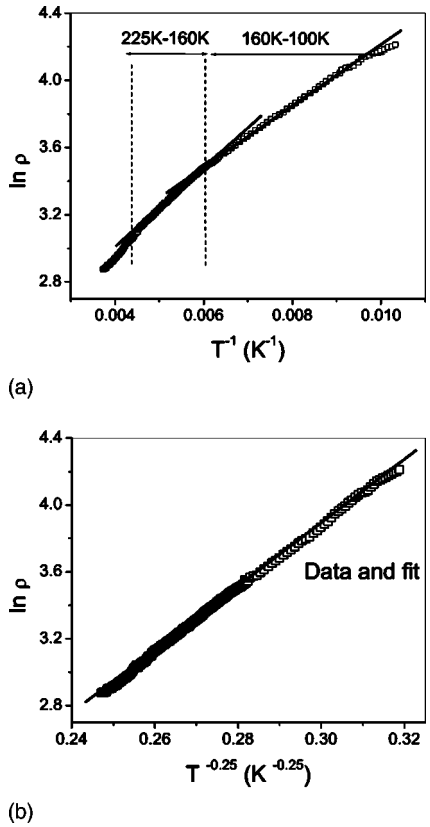

FIG. 3. For 1% N_2 sample plots show (a) activated behavior (b) variable range hopping conductivity.

theoretical value $(T_{1/4})^{1/4}=[5.7\alpha^3/kg_F]^{1/4}$.[9,13] The quantity $T_{1/4}$ is a measure or extent of the disorder and can be defined as an energy barrier between localized states. From Table II Ialthough a decrease of this quantity can be seen with the increase of N_2%, it is difficult to say whether g_F increases or (α decreases. A review on a similar kind of problem is presented in Ref. 16

Using the same formula hopping length is described as $R_{\text{hopp}}=(1/\alpha)\times(9/8\pi 1/5.7)^{1/4}\times(T_{1/4}/T)^{1/4}$.[9,13] This value of R_{hopp} is compared with $r_{\text{N-N}}$ and sometimes found inconsistent. The values are listed in Table II. The average energy for hopping $W=3/[4\pi {R_{\text{hopp}}}^3 g_F]$ and pre-exponential factor in conductivity is $\sigma_0=e^2 g_F {R_{\text{hopp}}}^2 \nu_{\text{ph}}=e^2\nu_{\text{ph}}[g_F/\alpha kT]^{1/2}$. The decrease of ρ_0 (i.e., increase of σ_0) with the increase of N_2% shows that there is an increase of DOS at the E_F provided the localization length (α^{-1}, a measure of the size of the sp^2 clusters in *a-C*) remains the same. Considering the value of ν_{ph} in the range between $10^{11}-10^{13}$ Hz the DOS has been calculated from the value of ρ_0 and it is found to be fairly consistent with the values calculated independently from $T_{1/4}$. The average energy available for hopping, a combined effect of g_F and R_{hopp}, is also found to increase with N_2%. This is an indication for the increase of the defect DOS in the samples with N_2% (up to 5% N_2) and is supported by the ESR results.

From Table II we see that for the 0.5% N_2 sample the hopping distance does not match with the nitrogen centers, which means VRH does not hold for this sample and an activated process can successfully explain the conductivity as described before. For 1 and 5 % N_2 samples the calculated hopping distances are reasonable. Results tabulated in Table II show that with the increase of nitrogen concentration average energy of hopping and DOS at E_F increase, whereas, the pre-exponential of resistivity, the constant $T_{1/4}$ and the hopping distance decrease. The DOS increases up to twice and R_{hopp} decreases up to four times with a change of nitrogen concentration by a factor of 3. For 5% N_2 samples R_{hopp} is about half of the distance between the nitrogen centers. This means hopping between carbon atoms also takes place. The increase of the DOS at the E_F is consistent with the increase of the ESR signal in the samples as the nitrogen concentration changes.

From the fitting of the temperature-dependent conductivity of the 1% N_2 sample, either the presence of soft gap (Coulomb gap) or a constant DOS at the E_F seems to be highly possible. Information obtained from these fits is tabulated in Tables II and III to verify which explanation is most appropriate in the present context. We look for supporting data such as frequency-dependent (ac) conductivity and linewidth variation of ESR peaks but a detailed study on ESR and ac conductivity will be given elsewhere.

ac conductivity can be expressed as $\sigma_{\text{ac}}=\sigma_{\text{dc}}+\sigma(\omega)$. The origin of ac conductivity is somewhat controversial and it is often thought that it arises from the relaxation processes due to hopping or tunneling of electrons or atoms between sites. A simple relationship is established between the ac conductivity and frequency $\sigma(\omega)=C\omega^s$, where $0\leqslant s\leqslant 1$, which generally holds well in the frequency range $10-10^7$ Hz, since this is determined by electronic hopping between defects or localized states.[9] For quantum mechanical tunneling the exponent "*s*" is independent of temperature and decreases with the increase of frequency unlike small and large polaron hopping or correlated barrier hopping of bi-polarons. In the case of small polaron tunneling the exponent s varies with temperature but we do not see any reason for the presence of

TABLE II. Calculated parameters based on Mott's VRH model of percolation.

N_2% (plasma)	N_{at} (cm^{-3})	$r_{\text{N-N}}$ (Å)	W (MeV)	ρ_0 (Ohm cm)	$(T_{1/4})^{1/4}$ K$^{1/4}$	g_F (cm^{-3} eV^{-1})	R_{hopp} (Å)
0.5	5.9×10^{19}	15.8	160	1.538	50.20 (233–277 K)	3.74×10^{20}	25.60 (250 K)
1.0	9.0×10^{19}	13.9	170	0.958	19.13 (280–80 K)	5.73×10^{20}	13.61 (200 K)
5.0	1.8×10^{20}	11.0	230	0.656	11.34 (300–160 K)	7.82×10^{20}	6.22 (200 K)

TABLE III. Calculated parameters based on Pollak's model of percolation and Coulomb gap.

N_2% (plasma)	R_{hopp}(Å)/VRH	$(T_{1/2})^{1/2}$ $K^{1/2}$	Δ (meV)	R_{hopp} Å(/Pollak)	E_m (meV)	E_H (meV)
1.0	13.6 (200 K)	19.1	99.0	6.75 (200 K)	120 (200 K)	24.9
5.0	6.22 (200 K)	7.816	115.6	2.69 (50 K)	50 (50 K)	23.2

small or large polarons in the present system unlike polymers or doped polymers. Also, the correlated barrier hopping of electrons has been observed in different kinds of systems such as V_2O_5-GeO_2 glasses and PbO-Fe_2O_3 glasses that are very different from our materials (also, verified from thermoelectric power measurement). As the present case is similar to tunneling and not other types of hopping we did not feel the importance of performing low-temperature ac conductivity of our samples. The pre-exponent C is expressed as $C=\pi N^2e^2/6kT(2\alpha)$ (α=polarizability of a pair of sites, N =number of sites per unit volume among which hopping takes place) depends weakly on temperature. Quantum mechanical tunneling of a carrier takes place through the potential barrier between the sites separated by a hopping distance R_ω. However, if the hopping distance between the centers is variable range in nature, then R_ω depends on frequency as given by $R_\omega=1/2\alpha\ln(1/\omega\tau_0)$ and the ac conductivity in terms of pair approximation is given by $\sigma(\omega)=Cg_F{}^2k_BTe^2\alpha^{-5}\omega\ln^4c(1/\omega\tau_0)$. The DOS ($g_F$) has been calculated from the fit of ac conductivity data that was found ($\sim 10^{20}$/eV cm^3) to be consistent with the dc conductivity measurements as described before.

The frequency component of the above equation is given by $s=d\ln\sigma(\omega)/d\ln\omega$ or $s=1-4\ln^{-1}(1/\omega\tau_0)$, where s is independent of temperature but not frequency and has the value ~ 0.8 for $\omega=10^4$ s^{-1} and $\tau_0=2\times10^{-13}$ s. Here τ_0 denotes the characteristic relaxation time and is of the order of the inverse phonon frequency. From this model electron tunneling "s" is predicted to be temperature independent but frequency dependent where the dielectric loss originates from the electronic relaxation and charge transfer occurs by the quantum mechanical tunneling through barriers. From the ln(conductivity) versus ln(frequency) [Fig. 4(a)] curve the value of the exponent is estimated to be ~ 0.9, which shows the possibility of the variable range hopping phenomena in the 1% N_2 sample [Fig. 4(a)].[9] In the samples prepared with high nitrogen (10% N_2) an opposite trend of conductivity with frequency (initially weak frequency dependence up to 500 kHz followed by a rapid decrease at high frequency range) can be observed and it did not follow VRH mechanism but a semimetallic nature [Fig. 4(a)].

Before showing the connection to the electrical conductivity we briefly describe the features of ESR measurement from the presently investigated samples. A typical Lorentzian shape of the ESR line is shown in the inset of Fig. 1(b), whose shape does not change significantly with nitrogen concentration. The samples prepared without nitrogen and with 1–5 % N_2 in the plasma showed high spin density ($10^{20}/cm^3$) that increases more than four times in the 5% N_2 samples compared to the 0% N_2 films [Fig. 1(b)]. Beyond that nitrogen level the spin density falls down with the nitrogen concentration in the plasma. For 20% N_2 sample the intensity of ESR signal has been found to be extremely weak. It was clearly seen that an increase of nitrogen percentage in the plasma enhances N_{at} in the films up to 5% N_2 in the plasma [Fig. 1(b)]. The absolute values of N atomic concentration and electron concentration (from Hall measurements)[14] and their trends do not coincide [Fig. 1(b)]. This discrepancy between the spin density and carrier concentration (n) may arise from the trapping of electrons by vacancy centers or high defect DOS. The spins most probably arise from the defect DOS and the complete analysis is underway. The Lande g value (2.0028) of the undoped and N-doped films is similar to diamondlike carbon films but different from tetrahedral amorphous carbon or high sp^2-rich films, which is mainly a signature of defect DOS and dangling bonds created by nitrogen incorporation. The variation of the spin density (or defect DOS) with nitrogen concentration in the plasma could explain the change of conductivity mechanism in these films and in good agreement with the previous analysis. For relatively low defect DOS (0.5% N_2 film) activated conduction, for relatively higher defect DOS (1% N_2 and 5% N_2 film s) hopping conduction and again for low defect DOS (>5% N_2 film) semimetallic or partial activated conduction (see the following discussions) at room temperature have been observed. Therefore, the conductivity

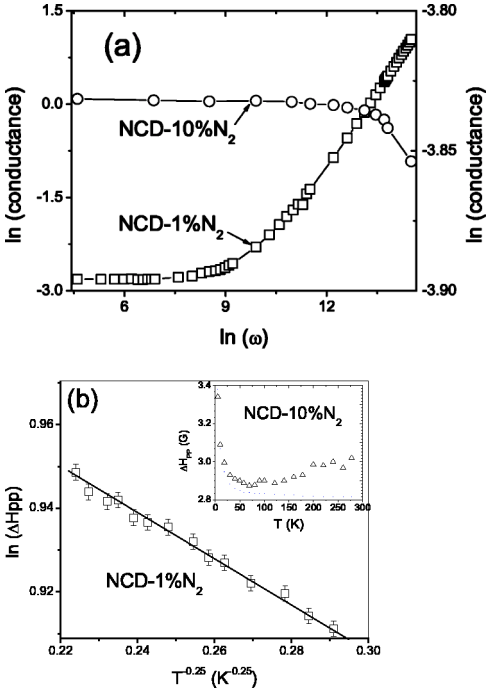

FIG. 4. (a) Variation of ln (conductivity) with ln (frequency) and (b) Variation of $\ln(\Delta H_{PP})$ with $T^{1/4}$ for 1% sample. The 1% N_2 film shows VRH fit. Inset: Variation of ΔH_{PP} with T for the 10% N_2 sample (Ref. 14).

path is shifted from E_F to the band edge with the change of defect DOS.

From the temperature dependence of the ESR linewidth (ΔH_{PP}) additional information concerning the dynamic effects can be found. Variation of the ΔH_{PP} with temperature can suggest the origin of conductivity, e.g., delocalization within sp^2-bonded clusters and intercluster hopping. Demichelis *et al.*[17] used an empirical formula to correlate the temperature dependence of electrical conductivity $[\sigma(T)]$ and ΔH_{PP} as $\Delta H_{PP}=\Delta H_{PP}(0)+C[\sigma(T)]^n$ where C and $\Delta H_{PP}(0)$ represent a constant and the linewidth at 0 K, respectively. It has been seen that for sputtered *a-C* films the best fit gave $\Delta H_{PP}(0)=2.3$ G and $n=0.32$.[17] This formula was previously used to relate the linewidth of dangling bond centers in *a*-Si with dc conductivity[17] and the decrease of the value of the exponent n with temperature was thought to originate from the hopping motion of the electrons, which is equivalent to the field fluctuation with time at the sites of the electrons.[17] For variable range hopping ΔH_{PP} varies as $\exp(-T_0/T)^{0.25}$. We should note that the change ΔH_{PP} of is an indirect measure of conductivity only. In the present case $\ln(\Delta H_{PP})$ showed a linear behavior with $T^{-0.25}$ confirming variable range hopping (VRH) conduction in 1% N_2 samples throughout the range of measurement [Fig. 4(b)]. Spin susceptibility (χ) of this weakly doped NCD film increases with the decrease of temperature and follows the Curie behavior. On the other hand for the 10% N_2 sample χ is weakly temperature dependent between 300 and 80 K but strongly temperature dependent below 80 K.[14] The important difference can be found in the variation of the ESR linewidth of 10% N_2 sample. ΔH_{PP} for 10% N_2 film does not follow the VRH fit [Fig. 4(b)]. This quantity initially decreases with the decrease of temperature down to 80 K and then rises up in the lower temperature regime [Fig. 4(b), Inset]. This behavior can be attributed to a very weakly Curie-type (above 50 K) or close to Paulitype. This trend is not truly supported by the hopping conduction mechanism[14] and provides a good indication of activated conduction at higher temperatures.

From Fig. 4(a) we find that the frequency dependent conductivity follows Mott's VRH hopping and δH_{PP} also follows a $T^{-0.25}$ dependence [Fig. 4(b)]. This supporting data leads us to consider that the temperature-dependent conductivity in the 1% N_2 films showed variable range hopping in 3D (i.e., $T^{-0.25}$ law) throughout the measured temperature range [Fig. 3(b)]. This can be explained by opening up some percolation path of the network or bridging by the impurities (suggested by previous models) that just crosses the percolation threshold. HRTEM images of the sample also showed a little increase of the width of GB in the films grown using 1% N_2 film compared to the undoped one.[1,14] The appearance of Mott's 3D VRH in the weakly doped NCD films (1% N_2) suggests that the localization length in these films is considerably shrunk due to the atomic scale disorder (see Sec. IV). For the films grown using 5% N_2 much wider GB have been noticed. Therefore, the percolation threshold has already been crossed. The $T^{-0.25}$ works in the low-temperature region, namely, 300 to 160 K, whereas, a $T^{-0.5}$ law $[\rho=\rho_0\exp(-T_{1/2}/T)^{0.5}]$ works over wider temperature range (15 to 100 K correspond to Efros hopping) [Figs. 5(a) and 5(b)]. According to Pollak's treatment[19] of the percolation model, DOS varies as $N(E)=N_0E^p$, where p is an exponent. Based on Pollak's model[19] Paillard *et al.*,[20] determined an analytical expression of $T_{1/2}$ as $T_{1/2}=7.4\ \alpha/kN_0^{1/3}$, where $N(E)=N_0E^2$. Following this treatment the energy from which conductivity starts $E_m=kT^{1/2}\ T_{1/2}{}^{1/2}$ and hopping distance $R=(1/4\alpha)\times(T_{1/2}/T)^{1/2}$ (where localization length $\alpha^{-1}=1$ nm) can be calculated. These values are compared with those obtained from Mott's VRH (see Table II).

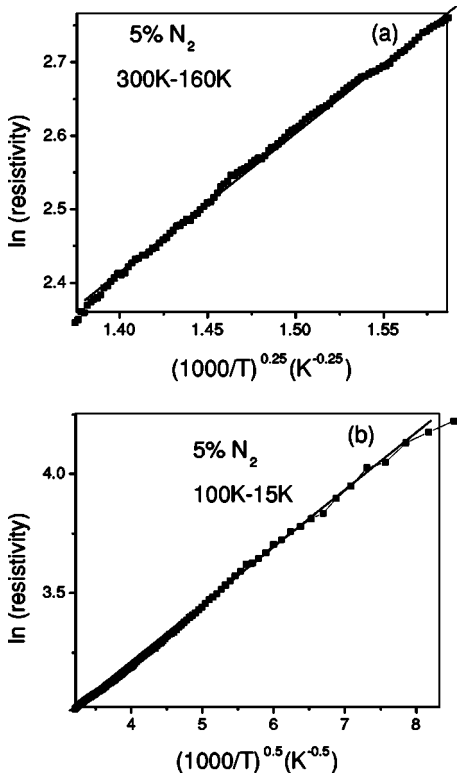

FIG. 5. Change over from Mott's VRH to Efros hopping with temperature in the 5% N_2 sample can be seen from the variation of the resistivity with (a) $T^{1/4}$ and (b) $T^{1/2}$ at different temperature ranges.

Applying percolation theory in this two-phase material we can think about a network resistance through the GB that connects the sites of localized states. The nitrogen atoms are acting as conducting sites and region of high conductivity, in which the localized states are connected by conductance more than the critical conductance of the network. The nitrogen sites are linked by nonconducting sp^3 sites. If the hopping distance decreases to a very small value due to the high concentration of the dopants the conductivity of the network exceeds the percolation limit and a very high conductivity would be seen. In addition little increase of sp^2-bonded carbon in the GB regions will also contribute to conductivity (see more discussions in the next section).

In case of the Coulomb interaction carrier correlation generates a gap (Coulomb gap) around the Fermi energy. The effect of Coulomb gap becomes effective when the thermal energy becomes sufficiently small compared to the width of the gap and it appears in the temperature region lower than the characteristic temperature $T_c\sim e^4N_0\ \alpha/k^2$, which is inversely proportional to the localization length. In the 5% N_2

film, there is a steep increase of the localization length and therefore, both T_c and $T_{1/2}$ decrease suggesting a possibility of $T^{0.5}$-type conductivity. The magnitude of Coulomb gap soft gap is given by the energy difference between two localized states depends on $(E-E_F)^2$ where DOS can be represented as $g(E)=g_0\,E^2$ with $g_0=(3/\pi k^3/e^6)$, where k is the dielectric constant. The magnitude of soft gap is given by $\delta=(g_F/g_0)^{1/2}$.[13] $E_m=KT^{1/2}$ $(T_{1/2})^{1/2}$ determines the energy range (relative to E_F) where conduction starts. From Table III it appears that for 5% N_2 sample conduction occurs very close (50 meV) to the Fermi level compared to the 1% N_2 sample (120 meV). The constant term in the expression $\rho=\rho_0[\exp(-T_{1/2}/T)^{1/2}]$ can be written as $T_{1/2}=e^2\beta\alpha/k_Bk$. The experimental value of $T_{1/2}$ obtained from the fit has been compared with the theoretical one. Finally, the soft gap can be deduced as $\Delta=(\pi g_F e^6/3k^3)^{1/2}$.[13] The value of hard gap E_H, is estimated as $\Delta/5$. It seems that both soft gap of 115 meV and hard gap of 23.2 meV are present in the DOS of the sample and they are observed at intermediate and low temperatures, respectively.

From Table III we notice that R_{hopp}(Pollak) is always lower than R_{hopp}(VRH). For the 1% N_2 sample R_{hopp}(Pollak) is very low and seems to be unacceptable. The values of the soft and hard gaps are comparable in the 1% N_2 and 5% N_2 sample. This result indicates that low temperature conductivity may show some finite value of soft and hard gap in the 10% N_2 sample and due to the limitation of the data this cannot be verified.

In the 10% N_2 film the temperature range of validity of Motts's VRH shifts towards lower values. The conductivity of the samples can be described as a combination of band conduction between 300 K and 250 K and hopping conduction between 270 K and 10 K. In this case linearity has been found in the range between 270 K and 125 K with $\exp T^{-0.25}$ fit. The presence of neither hard gap nor soft gap has been confirmed from this sample. A combination of delocalized state conduction (Arrhenious-type) and hopping conduction can nicely explain this temperature dependent conductivity. The total conductivity consists of the conduction band (CB) conductivity and the hopping conductivity $\sigma=\sigma_c+\sigma_h$. The CB conductivity is calculated with the formula $\sigma_c(T)=e\mu_c n_c(T)\equiv e\mu_c N_c(T)\exp[-(T)/kT]$, where μ_c represents the CB electron mobility (Fig. 6). We have taken chemical potential, μ (a measure of the shift of the Fermi level from the zero energy point) to be constant over the temperature variation since it varies slowly with temperature.[14] The expression for the hopping conductivity is $\sigma_h=\sigma_0\exp[-(T_{1/4}/T)^{1/4}]$, where $\sigma_0=e\mu_h p_2(T)$ and μ_h and $p_2(T)$ represent the hopping mobility and the concentration of electrons in another energy level say u_2. Thus the temperature dependence of the conductivity is determined by the coexistence of the band and hopping conductivities in a wide temperature range. To get the functional dependence of carrier concentration over temperature we plot the experimental data and use a nonlinear fit to get the formula (Fig. 6). $T_{1/4}$, σ_0, and $\mu(T)$ are taken as parameters whose values are found from the nonlinear fit.[14] A transition to the hopping conductivity for heavily doped NCD films can be explained as the temperature decreases the band conductivity with certain activation energy is observed

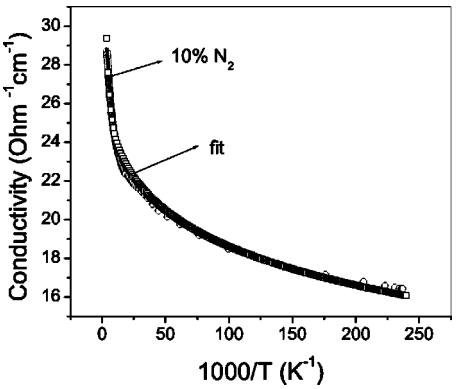

FIG. 6. Conductivity has been fitted with a combination of extended state and variable range hopping conduction in the 10% N_2 sample.

where only electrons thermally activated from the level u_2 participate in the conduction band conductivity. At the same time, the hopping conductivity in the level u_2 increases and at lower temperatures, when the thermal activation from the level u_2 becomes weak, hopping conduction becomes dominant.

From Fig. 6 it is clear that for the 10% N_2 sample the fit agrees well with the experimental results. Also, for 8.5 and 20 % N_2 samples this model holds very well (see the parameters in Table IV). Increase of σ_0, $T_{1/4}$, $\mu(T)$ with N_2% in the plasma can be found in Table IV. This means with nitrogen percentage carrier concentration, DOS, and shift of Fermi level from the mid gap towards conduction band increase. The amount of shift of E_F for the 20% N_2 sample is almost twice that of the 10% N_2 sample. This is one major conclusion in this article. Furthermore, increase in nitrogen concentration could lead to a semimetallic behavior because of the increase in the connectivity of sp^2 bonded carbon, higher delocalization of the π^* electronic states, and broadening of the π^* band. It can be suggested that some of the states in the gap might be quite delocalized and could form a new band similar to an impurity band (denoted as u_2) with its own mobility edges. Therefore, conductivity of samples prepared with high nitrogen percentage is fitted as a combination of band and hopping conduction. At high temperature band conduction prevails but at low temperature the contribution from thermally activated electrons from band u_2 decreases and hopping conduction dominates. Following our previous discussions regarding the 0.5% and 1% N_2 samples this features can be explained on the basis of the decrease of separation between the π bands. If this is the case at higher temperature conduction is due to carriers excited beyond the mobility shoulders into delocalized or extended states. On the other

TABLE IV. Calculated parameters based on the combined band and hopping conduction.

N_2% (plasma)	σ_0 (Ohm^{-1} cm^{-1})	$T_{1/4}$ (K$^{1/4}$)	μ(T) meV
8.5	15.56	160.1	35.2
10	33.96	190.3	47.4
20	206.01	283.1	84.1

hand, at the low-temperature regime carriers are excited into the localized states at the band edges therefore hopping of electrons takes place. Our model of combining activated (band tail conduction) and hopping (between neighboring graphitic islands or dimers in the present context) conduction at low and high temperatures, respectively, is also supported by the study of Dasgupta *et al.*[16] This kind of weak temperature-dependent conductivity was also found previously in highly conducting carbon films but not analyzed fully.[16] On the basis of Kubo's formula of dc conductivity Shimakawa and Miyake also suggested that as the DOS and mobility decrease with the decrease of energy, the conduction path shifts from the mobility edges towards the E_F as the temperature is lowered yielding nonactivated transport.[16] They also suggested that the tail state conduction could show high thermoelectric power and its strong temperature dependence[16] which was seen from the present samples.[14] Therefore hopping conduction at the tail states is possible in the present samples, which was seen in the low-temperature regimes. This problem would appear as complicated when we consider any interaction; e.g., electron-electron or electron phonon and will be discussed elsewhere. We have seen the effect of interaction when DOS is very high and hopping distance is very small. Moreover, due to the presence of more sp^2 bonded structure additional carriers will be generated that will turn the material into a metallic state.

IV. DISCUSSIONS: DOPING OF GRAIN BOUNDARIES

First we look at the GB of microcrystalline diamond and compare the transport properties with the present case. Malta *et al.*[16] attempted to establish the effect of grain boundaries on the conductivity in the *p*-doped diamond. Due to the effect of GB scattering mobility of carriers in microcrystalline diamond (MCD) can be significantly reduced compared to that in single crystal diamond. On the other hand, it was suggested that for heavily dopedmaterials, such as NCD, doped with nitrogen, the depletion of carriers would be much less and hence diamond GB should have a little effect on the transport properties.[21] Calculations, carried out by Kleblinsky *et al.*[22] and Zapol *et al.*,[23] showed GB playing a major role in the NCD films in current conduction. The structure of the GB is not totally disordered, and is at least very different from diamondlike carbon films. The GB regions are atomically thin and thus do not play any role for carrier scattering. Therefore, the role of GB in NCD is different from MCD films.

It is shown that when topological disorder is introduced and mostly confined to the two interface planes in the grain boundary regions between two diamond crystals, the electronic structure changes profoundly compared to bulk diamond.[24] We think that the electronic structure of the presently discussed thin GB is very different from the conventional $a-C$ films. For example, a number of electronic states appear in the band gap, which are π and π^* states on sp^2 carbon atoms as well as σ^* states associated with dangling bonds.[23,24] Also, nitrogen saturates the original dangling bonds and forms lone pairs instead. As opposed to the bulk, no bond breaking is required. The distortion of bonds is caused by the geometrical constraints due to the surrounding carbon lattice. These restrictions are weaker for nitrogen in the grain boundary compared to the diamond bulk because of the local disorder. Therefore, it is easier to accommodate nitrogen in the grain boundary. With the theoretical calculations indicating that nitrogen is favored by 3–5 eV for the doping of GB, a proposal that the nitrogen in these films is present predominantly in the GB and not within the grains has been made.[23] It was found at 1.5 eV below the valence-band maximum, and this state will be referred to as a lone pair. This will lead to an increase of the electron density at the Fermi level. The Fermi level will shift towards the conduction band, and this could result in the increase in *n*-type conductivity in UNCD films. The calculated values of shift of E_F for 10% N_2 and 20% N_2 samples are given in Table IV.

We can now consider the physical origin of hopping conduction in NCD grain boundaries. The effective energy gap or distance between π-π^* states in undoped NCD was estimated as 2.3 eV. Cleri *et al.*[25] suggested that even multiphonon assisted hopping conduction is possible in undoped NCD films with a conductivity of $\sim 10^{-6}$ $(\text{Ohm cm})^{-1}$ and but the average hopping length was not estimated. The value of the energy gap and conductivity is consistent with our measurement the hopping distance seems to be a few nanometers. It was suggested that hopping took place between sp^2 dimers across the grain boundary planes.[25] Although the structure of GB looks similar to graphite, the connectivity within GB is far from graphite as only a few dimers join into sp^2 chains of three and more atoms (see Ref. 25 for detailed structure of GB). Now the localized π states always occur in π-π^* pair around dimers rather that a single atom and π electrons hop to another dimer through an empty π^* state below the mobility edge. Due to the presence of a low dangling bond density, the ESR signal of undoped films is weaker than the doped films, which increases with nitrogen incorporation.

In undoped NCD films hopping takes place between dimers, i.e., perpendicular to the plane of GB making the hopping length small. However, due to lack of connectivity along the plane of GB conductivity is poor and measured hopping distance is large. This poor connectivity opens up a finite energy gap and an Arrhenious-type temperature-dependent conductivity can be expected. In weakly doped NCD film energy gap is reduced from 2.3 eV to a small finite value that can be measured by the present temperature-dependent conductivity and listed in Table I. This is seen from the 0.5% N_2 sample with a gap of 72 meV. On the other hand, if there is no energy gap and the DOS at E_F is large due to GB structure Mott's VRH would be expected[7] as is observed in the 1% N_2 sample. Nitrogen lone pair increases connectivity between carbon atoms along the plane of the GB and hopping takes place between nitrogen centers instead of dimers. This is similar to the case of quasi-one-dimensional filaments along which conductivity occurs. Also nitrogen forms states closer to E_F compared to the C=C band (2.3 eV) because it forms lone pair states. Therefore, primarily we can consider hopping between nitrogen centers along the plane of GB with hopping distance of 13 Å. Electrons taking part in hopping come from localized N centers or $C_3^- - N_4^+$ localized structure. Three bonds of N atom are

saturated one forms dangling bond and the rest of the electron hops to another N: center. Samples prepared with higher N_2% contain more dangling bonds. For 5% N_2 samples hopping distance is reduced to 6 Å, which is smaller than the distance between the nitrogen centers. Therefore, at that level hopping between nitrogen center to carbon center and also, carbon to carbon centers (energy level even closer to E_F) seem to be possible. These hypotheses can be supported by the present experimental observations such as the increase of conductivity without increase of nitrogen concentration in the samples [Fig. 1(b)]. Moreover, the hopping distance calculated from conductivity is lower than the average spacing between the nitrogen atoms [Table II].

In carbon there has been a debate on the conductivity path either at the E_F with constant DOS or at the band or mobility edges.[16] VRH has been recently revisited by Godet using a numerical model based on the calculation of the filling rate of empty electronic state where hopping characteristics were scaled with a product $g_F \times \alpha^{-3}$ and depending on the value of this product one could explain the characteristics of very weakly conducting samples having very low Hall mobility.[26] In this paper we confirm the validity of Mott's VRH using different consistent data and without making any further calculations. We plan to verify more carefully the validity of the Godet's model later, as that seems inapplicable for these samples having high conductivity and sufficient mobility.[26]

Next we make a comparison with boron-doped diamond. Boron-doped type-Ib synthetic diamond showed, in the doping density range 10^{18}–10^{19} cm^{-3}, an activation energy of 185 meV between 500 and 1000 K and around 368 meV between 300 and 500 K.[18] For a doping level lower than 10^{19} cm^{-3}, conduction process is governed by valence band conduction. For 2.5×10^{19} cm^{-3}, a new conduction process increases the conductivity at room temperature, which increases strongly with the boron concentration, as seen in the MCD films with a higher doping level and is attributed due to hopping between ionized and neutral acceptors within the impurity band. It has been suggested that hopping is of the nearest-neighbor hopping type (NNH). For a doping level of 2.7×10^{20} cm^{-3} or higher, the conductivity decreases with temperature suggesting a metallic behavior, in accordance with the Mott transition expected around 2×10^{20} cm^{-3}.[18] It is clearly seen that doping of grain boundary of NCD films is very different from electrical properties of B-doped diamond. Though electrical conductivity study has been performed in boron doped diamond using different kind of models[27] we think a true comparison can be made with B-doped NCD films but no reports are available.

Finally, we explain the transport properties of the GB of NCD films on the basis of the electronic structure of amorphous carbon.[28] Amorphous carbon films can be distinguished into two categories where a finite energy gap is either present or absent and they are found to manifest entirely different temperature-dependent conductivity. Now for gapless *a-C* when the band edges overlap the states at the E_F can be either localized or delocalized. In the case of overlapping states the effective energy gap or activation energy is a measure of the distance between the mobility edges or the width of the localized states having no conductivity. For gapless *a-C* films these are localized π states (or π defects) at the E_F and its width depends on the degree of disorder of sp^2 bonded carbon and folding of rings that controls the conductivity mechanism such as the hopping conduction at the E_F (semimetallic with negative temperature dependence of resistivity) or delocalized conduction for no π defects (metallic with positive temperature dependence of resistivity as in graphite). On the other hand, when the concentration or effect of π bonds is relatively small a finite gap in *a-C* films appears. This contributes solely to hopping conductivity (of relatively high conductivity) close to E_F or activated conductivity at the bands edges. With the change of temperature, conduction shifts from E_F to the band tails states and as a result the slope of temperature-dependent conductivity curve changes producing a transition between localized and delocalized state conductivity.

Keeping in mind the previous discussion when we first look at the more conducting samples (prepared with 8.5–20% N_2) and find that they behave similar to a gapless *a-C* films where a combination of activated (high temperature) and hopping (low temperature) conduction explains the whole temperature range of conductivity. All these curves corresponding to the nitrogen concentration 8.5–20% N_2 look similar except for a shift in the conductivity scale. With N_2% the concentration of sp^2 bond increases and the amount of localization reduces, so the width of localized states decreases with structural change. Notice that the reduction of spin density with nitrogen concentration beyond 5% in the plasma. Now the reason behind the increase of the absolute value of conductivity (at a particular temperature) with N_2% in the plasma is the increase of mobility and carrier concentration in the extended (band) states (also these two quantities increase with energy or temperature as they are energy dependent). Interestingly there is hardly any change in the hopping mobility or hopping conductivity with N_2% in these metallic samples.

We think that the temperature dependent conductivity of the 5% N_2 film just show a continuous transition between these two phases, gap ($<5\%$ N_2) or no gap ($>5\%$ N_2), which is rarely observed so well in this kind of films. In this sample we see the presence of soft or Coulomb gap and a hard gap and these features are entirely different from the 8.5, 10 % N_2 samples such as delocalized conduction at high temperature and hopping conduction at low temperature. This dependence for 5% N_2 is just the reverse, i.e., hopping at high temperature (hopping at band tail state not at the E_F) and $T^{-0.5}$ or T^{-1} dependence at low temperatures (DOS at the E_F is very low or absent). For the 1% N_2 sample hopping at the band state also takes place and for 0.5% N_2 mostly activated conduction works establishing the presence of an energy gap in these films. Notice again the decrease of the defect DOS (spin density) from 5% N_2 to 0.5% N_2 sample. In other words an increase of the defect DOS enhances the conductivity in 0.5–5 % N_2 samples. This effect is similar to other amorphous semiconductors such as *a*-Si:H where a large change of the conducting curves can be seen with dopant concentration and not by the change of structure. Thus we connect the transport in NCD films in the main flow of conductivity of amorphous carbon and related materials showing the special effect of sp^2 defects at the E_F and the width of localized states (π defects).

V. CONCLUSION

In summary we can say that the 0.5% N_2 sample (having low N concentration) shows predominantly Arrhenious-type behavior with a distinct change in activation energy at different temperatures. The presence of a hard gap is confirmed in the sample having a low concentration of nitrogen. For 1% N_2, the sample shows Arrhenious behavior at a very limited temperature range but the data agree in the entire temperature range for both Pollok and Mott's model. The question which model is more appropriate has been resolved by supporting data that confirms Mott's VRH throughout the temperature range. It is suggested that nitrogen induces percolative paths in the GB regions and therefore increases the conductivity. The DOS at the E_F increases with N_2% in the plasma. For the 5% N_2 sample, a Coulomb gap was observed. The 5% N_2 sample obeys Pollok's model in the low-temperature range (85–15 K) and Mott's model in the range 300–160 K. For higher N_2% conductivity can be expressed as a combination of delocalized state conduction and hopping conduction where a shift of E_F towards CB has been noticed. These experimental observations are in agreement with theoretically predicated electronic structure and properties of these materials. Also, the typical problem of analysis of temperature-dependent conductivity data of amorphous carbon is attempted to resolve by the present approach.

ACKNOWLEDGMENTS

The author would very much like to thank D. M. Gruen, A. R. Krauss, J. J. Schlueter, H. Wang, and other group members of Argonne National Laboratory for various help including synthesis and some of the characterizations of the NCD samples. S. Bhattacharyya, D. Banerjee, and S. Samui are also acknowledged for their help to perform this work.

[1] S. Bhattacharyya, O. Auciello, J. Birrel, J.A. Carlisle, L.A. Curtiss, A.N. Goyette, D.M. Gruen, A.R. Krauss, J. Schlueter, A. Sumant, and P. Zapol, Appl. Phys. Lett. **79**, 1441 (2001).

[2] Th. Frauenheim, G. Jungnickel, P. Stich, M. Kaukonen, F. Weich, J. Widnay, and D. Porezag, Diamond Relat. Mater. **7**, 348 (1998).

[3] S. A. Kajihara, A. Antonelli, J. Bernholc, and R. Car, Phys. Rev. Lett. **66**, 2010 (1991).

[4] E. Rohrer, C. F. O. Graeff, R. Janssen, C. E. Nebel, H. Guettler, and R. Zachai, Phys. Rev. B **54**, 7874 (1996).

[5] D. R. Mckenzie, D. A. Muller, and B. A. Paithorpe, Phys. Rev. Lett. **67**, 773 (1991).

[6] J. Robertson and C. A. Davis, Diamond Relat. Mater. **4**, 441 (1995).

[7] C. Ronning, U. Griesmeier, M. Gross, H. C. Hofsäss, R. G. Downing, and G. P. Lamaze, Diamond Relat. Mater. **4**, 666 (1995).

[8] B. Massarani, J. C. Bourgoin, and R. M. Chrenko, Phys. Rev. B **17**, 1758 (1978).

[9] N. F. Mott and E. A. Davis, in *Electronic Processes in Non-Crystalline Solids* (Clarendon Press, Oxford, 1979); S. R. Elliot, *Physics of Amorphous Materials*, 2nd ed. (Longman, London, 1990).

[10] A. L. Efros and B. I. Shklovskii, J. Phys. C **8**, L49 (1975); **9**, 2021 (1976).

[11] M. Pollak, Philos. Mag. B **65**, 657 (1992).

[12] P. Dai, Y. Zhang, and M. P. Sarachik, Phys. Rev. Lett. **69**, 1804 (1992).

[13] T. Sato, K. Ohashi, H. Sugai, T. Sumi, K. Haruna, H. Maeta, N. Matsumoto, and H. Otsuka, Phys. Rev. B **61**, 12 970 (2000).

[14] T. Sharda and S. Bhattacharyya, in *Encyclopedia of Nanoscience and Nanotechnology*, edited by H. S. Nalwa (American Scientific Publishers, 2004), Vol 2, pp. 337–370; S. Bhattacharyya, presented at MRS-Fall meeting, 2000 (unpublished).

[15] S. Koizumi, M. Kamo, Y. Sato, H. Ozaki, and T. Inuzuka, Appl. Phys. Lett. **71**, 1065 (1999); I. Sakaguchi, M. N. -Gamo, Y. Kikuchi, E. Yasu, H. Haneda, T. Suzuki, and T. Ando, Phys. Rev. B **60**, R2139 (1999); E. P. Visser, G. J. Bauhuis, G. Janssen, W. Vollenberg, W. J. P. van Enckevort, and L. J. Giling, J. Phys.: Condens. Matter **4**, 7365 (1992).

[16] A. Helmbold, P. Hammer, J. U. Thiele, K. Rohwer, and D. Meissner, Philos. Mag. B **72**, 35 (1995); M. Koos, S. H. S. Moustafa, E. Szilagyi, and I. Pocsik, Diamond Relat. Mater. **8**, 1919 (1999); D. Dasgupta, F. Demichelis, and A. Tagliaferro, Philos. Mag. B **63**, 1255 (1991); K. Shimakawa, and K. Miyake, Phys. Rev. B **39**, 7578 (1989).

[17] F. Demichelis, C. De Martino, A. Tagliaferro, and M. Fanciculli, Diamond Relat. Mater. **3**, 844 (1994); U. Voget-Grove, J. Stuke, and H. Wagner (unpublished); B. Movagher, L. Schweitzer, and H. Overhof, Philos. Mag. B **37**, 683 (1978).

[18] K. J.-P. Lagrange, A. Deneuville, and E. Gheeraert, Diamond Relat. Mater. **7**, 1390 (1998); E. Broitman *et al.*, J. Appl. Phys. **89**, 1184 (2001); M. Ricci *et al.*, J. Mater. Sci. **8**, 480 (1993).

[19] M. Pollak, J. Non-Cryst. Solids **11**, 1 (1972).

[20] V. Paillard, M. Meaudre, P. Melinon, V. Dupuis, J. P. Perez, S. Vignoli, A. Perez, and R. Meaudre, J. Non-Cryst. Solids **191**, 174 (1995).

[21] K. Nihimura, K. Das, and J. T. Glass, J. Appl. Phys. **69**, 3142 (1991).

[22] P. Kleblinski, S. R. Phillpot, D. Wolf, and H. Gleiter, Nanostruct. Mater. **12**, 339 (1999).

[23] P. Zapol, M. Sternberg, L. A. Curtiss, T. Frauenheim, and D. M. Gruen, Phys. Rev. B **65**, 045403 (2001).

[24] D. M. Gruen, P. C. Redfern, D. A. Horner, P. Zapol, and L. A. Curtiss, J. Phys. Chem. **103**, 5459 (1999).

[25] F. Cleri, P. Keblniski, L. Colombo, D. Wolf, and S. R. Phillpot, Europhys. Lett. **46**, 671 (1999).

[26] C. Godet, Diamond Relat. Mater. **12**, 159 (2003); J. Non-Cryst. Solids **299**, 333 (2002); Phys. Status Solidi B **231**, 499 (2002).

[27] T. Inushima, T. Matsushita, S. Ohya, and H. Shiomi, Diamond Relat. Mater. **9**, 1066 (2000).

[28] S. Bhattacharyya and S. V. Subramanyam, *Electrical and Optical Polymer Systems: Fundamentals, Methods and Applications*, edited by Donald L. Wise (Marcel Dekker, New York, 1998), pp. 201–296.